

# Reduced-Complexity SFBC-OFDM for Vehicular Channels with High Mobility

Ahmed A. Abotabl, Amr El-Keyi, Yahya Mohasseb, and Tamer ElBatt

Wireless Intelligent Networks Center (WINC), Nile University, Cairo, Egypt.

ahmed.atyia@nileu.edu.eg, {aelkeyi, ymohasseb, telbatt}@nileuniversity.edu.eg

**Abstract**—Space frequency block coding with orthogonal frequency division multiplexing (SFBC-OFDM) suffers from the effect of inter-carrier interference (ICI) in doubly-selective communication channels. In this paper, a scheme is proposed in which windowing is applied to the received signal to reduce the effect of ICI to a limited number of neighboring sub-carriers. The sub-carriers holding the SFBC components of each codeword are separated by a number of sub-carriers larger than the ICI range, and hence, they do not interfere with each other. In order to preserve the structure of the SFBC, the separation between the codeword components is also selected within the coherence bandwidth of the channel. As a result, the diversity gain of the SFBC is preserved. A decision feedback equalizer is proposed to estimate the transmitted data symbols with low complexity. Simulation results are presented showing the ability of the proposed scheme to significantly improve the performance of SFBC-OFDM and preserve its diversity gain.

## I. INTRODUCTION

Vehicular communication systems are characterized by their challenging channel that is doubly-selective in both time and frequency [1]. Orthogonal frequency division multiplexing (OFDM) [2] has been selected as the modulation scheme in the 802.11p protocol for wireless access in vehicular environments (WAVE) due to its ability to handle frequency-selective channels. In OFDM, the number of sub-carriers,  $N$ , is selected such that the frequency-selective channel is decomposed into a set of parallel non-interfering frequency flat channels. In order for OFDM-based systems to operate properly, the channel impulse response has to be constant over the OFDM symbol duration. However, in time-selective channels that are not quasi-static over the OFDM symbol duration, inter-carrier interference (ICI) arises and the orthogonality between the OFDM sub-carriers is lost. Complete removal of ICI in OFDM systems requires the inversion of an  $N \times N$  channel matrix which might be computationally prohibitive. In order to combat this problem, the authors of [3] proposed a finite impulse response minimum mean square error (MMSE) equalizer with few (typically three) taps per sub-carrier. Also, a low complexity equalizer for OFDM signals was proposed in [4] by applying a window that maximizes the signal to interference (due to ICI) ratio.

Reliability is an important requirement for vehicular communications especially for safety applications. Employing multiple antennas at the transmitting and/or receiving vehicle

allows the use of spatial diversity techniques [5]. Space-frequency block coding (SFBC) maps the components of each codeword across antennas and different sub-carriers within the same OFDM symbol [6]. Hence, it requires the channel to be constant during one OFDM symbol only. However, when the channel varies during the OFDM symbol duration, the resulting ICI destroys the structure of the SFBC scheme resulting in loss of the diversity gain. The authors of [7] proposed separating the sub-carriers holding the codeword components within the coherence bandwidth to reduce the effect of ICI. Nevertheless, in vehicular channels with high mobility and small coherence bandwidth, the ICI would still have significant effect on the diversity gain.

In this paper, we propose an SFBC-OFDM design technique for doubly-selective channels encountered in vehicular communication systems. In the proposed scheme, the received OFDM symbol is multiplied by a window to limit the ICI to a small number of neighboring sub-carriers [4]. The window is designed to minimize the ICI power outside a certain adjustable range of neighboring sub-carriers while preserving the total energy of the received signal. As a result, a small separation between the codeword components is enough to reduce the interference from these components on each other where the separation need to be only larger than the range of ICI. The separation is also selected smaller than the coherence bandwidth of the channel to guarantee that the SFBC codeword components are subjected to the same channel. As a result, the proposed scheme provides higher immunity against fading channels with severe temporal and frequency selectivity. Due to the design of the window, the data symbol is divided into a number of sub-symbols where each sub-symbol is equalized/decoded independently. We design a minimum mean square error (MMSE)-based decision feedback equalizer (DFE) to decode the sub-symbols that takes into account the coloring effect of the window on the white noise. Simulation results show that the proposed scheme can provide high diversity even in channels with high Doppler shift.

## II. SYSTEM MODEL

We consider the SFBC-OFDM system shown in Fig. 1. For the sake of simplicity, we focus on the Alamouti coding scheme with two transmit antennas and a single receive antenna. Nevertheless, the proposed design can be extended to any orthogonal SFBC technique. Let the  $N \times 1$  vector  $\mathbf{d} = [d_0, d_1, \dots, d_{N-1}]^T$  denote the baseband modulated

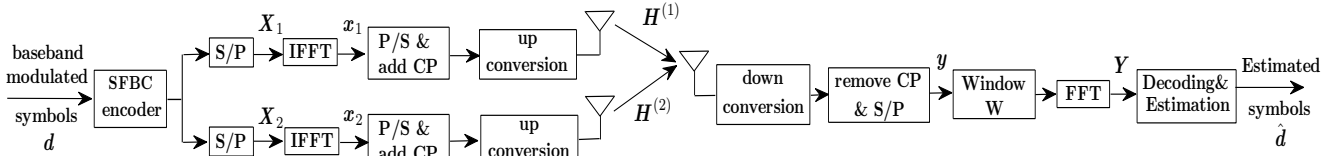


Fig. 1:  $2 \times 1$  SFBC transmitter and receiver.

data symbols where  $N$  is the number of sub-carriers per OFDM symbol, and  $(\cdot)^T$  and  $(\cdot)^H$  denote the transpose and Hermitian transpose operators, respectively. The baseband modulated symbols  $\mathbf{d}$  are Alamouti-coded across the two antennas using the OFDM sub-carriers instead of time slots. The two components of the Alamouti codeword are separated by  $L$  sub-carriers as shown in Fig. 2. For example, the components of the first codeword,  $[d_0 \ d_1]^T$  and  $[-d_1^* \ d_0^*]^T$ , are transmitted on sub-carriers 0 and  $L$ , respectively where  $(\cdot)^*$  denotes the complex conjugate. The separation is selected to be smaller than the coherence bandwidth of the channel to guarantee that the channel is almost constant across the codeword components [7].

The output of the SFBC encoder is the two  $N \times 1$  vectors  $\mathbf{X}_1$  and  $\mathbf{X}_2$  that represent the frequency-domain OFDM symbols transmitted from each antenna. They are given by

$$\mathbf{X}_1 = \mathbf{P}_1 \mathbf{d} - \bar{\mathbf{P}}_1 \mathbf{d}^* \quad (1)$$

$$\mathbf{X}_2 = \mathbf{P}_2 \mathbf{d} + \bar{\mathbf{P}}_2 \mathbf{d}^* \quad (2)$$

where the  $N \times N$  matrices  $\mathbf{P}_1$ ,  $\bar{\mathbf{P}}_1$ ,  $\mathbf{P}_2$  and  $\bar{\mathbf{P}}_2$  are given by

$$\mathbf{P}_1 = \mathbf{I}_{\frac{N}{2L}} \otimes \begin{bmatrix} \mathbf{V} \\ \mathbf{0}_{L \times 2L} \end{bmatrix}, \quad \bar{\mathbf{P}}_1 = \mathbf{I}_{\frac{N}{2L}} \otimes \begin{bmatrix} \mathbf{0}_{L \times 2L} \\ \bar{\mathbf{V}} \end{bmatrix},$$

$$\mathbf{P}_2 = \mathbf{I}_{\frac{N}{2L}} \otimes \begin{bmatrix} \mathbf{0}_{L \times 2L} \\ \mathbf{V} \end{bmatrix}, \quad \bar{\mathbf{P}}_2 = \mathbf{I}_{\frac{N}{2L}} \otimes \begin{bmatrix} \bar{\mathbf{V}} \\ \mathbf{0}_{L \times 2L} \end{bmatrix}$$

where  $\mathbf{I}_K$  denotes the  $K \times K$  identity matrix,  $\otimes$  denotes the Kronecker product,  $\mathbf{0}_{m,n}$  denotes an all zeros matrix of size  $m \times n$  and  $\mathbf{V}$  and  $\bar{\mathbf{V}}$  are the  $L \times 2L$  matrices containing the odd and even rows of the matrix  $\mathbf{I}_{2L}$  respectively.

Note that the two OFDM symbols  $\mathbf{X}_1$  and  $\mathbf{X}_2$  contain  $N/2$  Alamouti codewords as shown in Fig. 2. The two symbols are then converted to the time-domain symbols  $x_1$  and  $x_2$  using an  $N$ -point IFFT operation. The cyclic prefix is then added with length equal to or larger than the length of the channel impulse response to prevent inter-symbol interference. The received symbol after removing the cyclic prefix is given by

$$\mathbf{y} = \mathbf{H}^{(1)} \mathbf{x}_1 + \mathbf{H}^{(2)} \mathbf{x}_2 + \mathbf{u} \quad (3)$$

where  $\mathbf{H}^{(i)}$  is the  $i$ th time-domain channel matrix between the  $i$ th transmit antenna and the receiver and  $\mathbf{u}$  is the time-domain noise vector. The noise is white circular Gaussian with zero mean and covariance  $\sigma^2 \mathbf{I}_N$ .

In the conventional OFDM receiver, the received time-domain vector  $\mathbf{y}$  is converted to the frequency-domain vector  $\mathbf{Y}$  using an  $N$ -point FFT operation to obtain

$$\mathbf{Y} = \mathbf{G}_c^{(1)} \mathbf{X}_1 + \mathbf{G}_c^{(2)} \mathbf{X}_2 + \mathbf{U}_c \quad (4)$$

where  $\mathbf{G}_c^{(i)}$  is the  $i$ th frequency-domain channel matrix, i.e.,  $\mathbf{G}_c^{(i)} = \mathbf{F} \mathbf{H}^{(i)} \mathbf{F}^H$ , the  $N \times N$  matrix  $\mathbf{F}$  is the unitary discrete Fourier transform matrix, and  $\mathbf{U}_c$  is the frequency-domain noise vector, i.e.,  $\mathbf{U}_c = \mathbf{F} \mathbf{u}$ .

In quasi-static channels where the channel is constant over the OFDM symbol duration, the matrix  $\mathbf{H}^{(i)}$  is circulant and the matrix  $\mathbf{G}_c^{(i)}$  is a diagonal matrix. In this case, the Alamouti codeword components are orthogonal yielding the maximum diversity gain. Also, decoding is simple since  $\mathbf{G}_c^{(i)}$  is diagonal. However, when temporal selectivity arises, the channel matrix  $\mathbf{H}^{(i)}$  is not circulant, and hence,  $\mathbf{F} \mathbf{H}^{(i)} \mathbf{F}^H$  is not diagonal. Since the ICI is strongest for immediately neighboring sub-carriers, the code components are separated to reduce mutual ICI as in [7]. yet, this might not be sufficient to completely remove the ICI.

### III. MAXIMUM SIR WINDOW DESIGN

In this work, we focus on mitigating/exploiting the double selectivity of the channel as in [4] and do not consider the channel estimation problem. Hence, we assume that the receiver has an accurate estimate of the channel state, and hence, the matrices  $\mathbf{H}^{(1)}$  and  $\mathbf{H}^{(2)}$  are known. We propose the use of interference suppression by reducing the range of interference of each sub-carrier as in [4]. As a result, a smaller separation between the codeword components is sufficient to limit the ICI, and hence, the proposed scheme can accommodate communication channels with high temporal and frequency selectivity.

The windowing is performed by multiplying the time-domain received signal vector  $\mathbf{y}$  by the  $N \times N$  diagonal matrix  $\mathbf{W}$  as shown in Fig. 1 which will be specified later. As a result, the received frequency-domain vector becomes

$$\mathbf{Y} = \mathbf{G}^{(1)} \mathbf{X}_1 + \mathbf{G}^{(2)} \mathbf{X}_2 + \mathbf{U} \quad (5)$$

where the equivalent frequency-domain channel matrix  $\mathbf{G}^{(i)}$  is given by  $\mathbf{G}^{(i)} = \mathbf{F} \mathbf{W} \mathbf{H}^{(i)} \mathbf{F}^H$  and the  $N \times 1$  vector  $\mathbf{U}$  represents the equivalent frequency-domain noise vector, i.e.,  $\mathbf{U} = \mathbf{F} \mathbf{W} \mathbf{u}$ . The applied window is designed to modify the conventional frequency-domain channel matrices to have a structure as shown in Fig. 3 where the entries in the unshaded region have insignificant values and  $t$  is a design parameter that controls the size of the shaded region. The elements of  $\mathbf{G}^{(i)}$  that lie within the unshaded region in Fig. 3 are considered non-desired “interference” components whereas the shaded entries can be considered as the “desired signal” components.

Similar to the case in [4], the window is designed to maximize the signal to interference ratio (SIR) which is

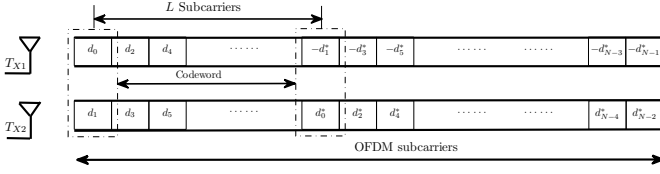


Fig. 2: Alamouti SFBC with separation across sub-carriers.

defined as the ratio between the energy contained in the desired signal components,  $E_s$ , and that contained in the interference components,  $E_I$ . The signal energy can be expressed in terms of the window using matrix notation as in [4] as

$$E_s = \sum_{i=1}^2 \|\mathbf{P}\mathbf{F}\mathbf{W}\mathbf{F}^H\mathbf{D}^{(i)}\|_F^2 \quad (6)$$

where  $\|\cdot\|$  denotes the Frobenius norm of a matrix and  $\mathbf{D}^{(i)}$  is a rearrangement of  $\mathbf{G}_c^{(i)}$  defined by

$$\mathbf{D}^{(i)}(m, n) = \mathbf{G}_c^{(i)}(\langle m + n - 2 \rangle_N, n),$$

where  $\mathbf{X}(m, n)$  is the element in the  $m$ th row and  $n$ th column of the matrix  $\mathbf{X}$ ,  $\langle \cdot \rangle_N$  denotes the modulo- $N$  operator and the  $N \times N$  matrix  $\mathbf{P}$  is given by

$$\mathbf{P} = \begin{bmatrix} \mathbf{I}_t & \mathbf{0} & \mathbf{0} \\ \mathbf{0} & \mathbf{0} & \mathbf{0} \\ \mathbf{0} & \mathbf{0} & \mathbf{I}_{t-1} \end{bmatrix}. \quad (7)$$

Using the identity  $\|\mathbf{X}\|_F^2 = \text{tr}\{\mathbf{X}\mathbf{X}^H\}$ , where  $\text{tr}\{\mathbf{X}\}$  is the trace of the matrix  $\mathbf{X}$  and noting that  $\mathbf{P}\mathbf{P}^H = \mathbf{P}$ , we can write  $E_s$  as

$$E_s = \sum_{i=1}^2 \text{tr} \left\{ \mathbf{P}\mathbf{F}\mathbf{W}\mathbf{F}^H\mathbf{D}^{(i)} \left( \mathbf{F}\mathbf{W}\mathbf{F}^H\mathbf{D}^{(i)} \right)^H \right\} \quad (8)$$

Note that multiplying a matrix from the left by the matrix  $\mathbf{P}$  in (7) nulls all the elements of the matrix except the first  $t$  and last  $t-1$  rows. After some mathematical manipulations, we can write (8) as

$$E_s = \mathbf{w}^H \mathbf{R}_S \mathbf{w} \quad (9)$$

where the  $N \times 1$  vector  $\mathbf{w}$  contains the diagonal elements of  $\mathbf{W}$  and the  $N \times N$  matrix  $\mathbf{R}_S$  is given by

$$\mathbf{R}_S^T = \sum_{i=1}^2 \sum_{j \in \mathcal{S}_t} \text{diag}\{\mathbf{f}_j\} (\mathbf{F}^H \mathbf{D}^{(i)}) (\mathbf{F}^H \mathbf{D}^{(i)})^H \text{diag}\{\mathbf{f}_j^*\}$$

where  $\mathbf{f}_k$  is the  $k$ th column of  $\mathbf{F}$  and  $\text{diag}\{\mathbf{x}\}$  is a diagonal matrix with the vector  $\mathbf{x}$  on its main diagonal. The inner summation is performed over values of  $j$  that belong to the set  $\mathcal{S}_t = \{j\}_1^t \cup \{j\}_{N-t+2}^N$ , i.e., it contains  $2t-1$  terms.

Next, we express the interference energy,  $E_I$ , in terms of the diagonal elements of the window. The interference energy can be written as  $E_I = E_T - E_s$  where  $E_T$  represents the total energy of the desired signal terms and the interference terms. The total energy is given by the sum of the squares of the Frobenius norms of the two matrices  $\mathbf{G}^{(1)}$  and  $\mathbf{G}^{(2)}$ , i.e.,

$$E_T = \sum_{i=1}^2 \text{tr} \left\{ \mathbf{W} \mathbf{H}^{(i)} \mathbf{H}^{(i)H} \mathbf{W}^H \right\}. \quad (10)$$

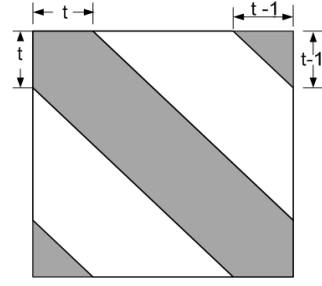


Fig. 3: Banded structure of the equivalent channel matrices  $\mathbf{G}^{(1)}$  and  $\mathbf{G}^{(2)}$  after applying the window.

Due to the diagonal structure of the matrix  $\mathbf{W}$ ,  $E_T$  can be expressed in terms of the vector  $\mathbf{w}$  that contains the diagonal elements of  $\mathbf{W}$  as

$$E_T = \mathbf{w}^H \mathbf{R}_T \mathbf{w} \quad (11)$$

where the  $N \times N$  diagonal matrix  $\mathbf{R}_T$  contains the main diagonal of the matrix  $\sum_{i=1}^2 \mathbf{H}^{(i)} \mathbf{H}^{(i)H}$  on its main diagonal.

Using (9) and (11), and introducing the  $N \times 1$  vector  $\tilde{\mathbf{w}} = \mathbf{R}_T^{-\frac{1}{2}} \mathbf{w}$ , we can write the SIR as

$$\text{SIR} = \frac{\tilde{\mathbf{w}}^H \mathbf{R}_T^{-\frac{1}{2}} \mathbf{R}_S \mathbf{R}_T^{-\frac{1}{2}} \tilde{\mathbf{w}}}{\|\tilde{\mathbf{w}}\|^2 - \tilde{\mathbf{w}}^H \mathbf{R}_T^{-\frac{1}{2}} \mathbf{R}_S \mathbf{R}_T^{-\frac{1}{2}} \tilde{\mathbf{w}}}. \quad (12)$$

Since the above expression for the SIR is invariant to multiplying the vector  $\tilde{\mathbf{w}}$  by a scalar, we can set  $\|\tilde{\mathbf{w}}\|^2 = 1$  without any loss of generality. Hence, the window design problem can be formulated as

$$\max_{\tilde{\mathbf{w}}} \frac{\tilde{\mathbf{w}}^H \mathbf{R}_T^{-\frac{1}{2}} \mathbf{R}_S \mathbf{R}_T^{-\frac{1}{2}} \tilde{\mathbf{w}}}{1 - \tilde{\mathbf{w}}^H \mathbf{R}_T^{-\frac{1}{2}} \mathbf{R}_S \mathbf{R}_T^{-\frac{1}{2}} \tilde{\mathbf{w}}} \quad \text{s.t.} \quad \|\tilde{\mathbf{w}}\|^2 = 1 \quad (13)$$

Note that both the numerator and denominator of the cost function are nonnegative. Since the function  $f(x) = x/(1-x)$  is monotonically increasing for  $0 \leq x < 1$ , the solution to the above problem is the unit-norm vector that maximizes the numerator of the objective function, i.e., the eigen vector associated with the maximum eigen value of the matrix  $\mathbf{R}_T^{-\frac{1}{2}} \mathbf{R}_S \mathbf{R}_T^{-\frac{1}{2}}$ . Hence, the vector  $\mathbf{w}$  is given by

$$\mathbf{w} = \mathbf{R}_T^{-\frac{1}{2}} \boldsymbol{\nu} \left\{ \mathbf{R}_T^{-\frac{1}{2}} \mathbf{R}_S \mathbf{R}_T^{-\frac{1}{2}} \right\} \quad (14)$$

where  $\boldsymbol{\nu}\{\mathbf{X}\}$  denotes the eigen vector associated with the maximum eigen value of the matrix  $\mathbf{X}$ .

Since the matrix  $\mathbf{R}_T$  is diagonal, evaluating  $\mathbf{R}_T^{-\frac{1}{2}} \mathbf{R}_S \mathbf{R}_T^{-\frac{1}{2}}$  requires only  $\mathcal{O}(N^2)$  operations. Also, the computational complexity of finding the maximum eigen vector of an  $N \times N$  matrix is of  $\mathcal{O}(N^2)$ . Therefore, the computational complexity of finding the window is of  $\mathcal{O}(N^2)$ . Note that this computational complexity is much less than the complexity of the MMSE equalizer that requires the inversion of an  $N \times N$  matrix.

#### IV. DECISION FEEDBACK EQUALIZER

Decoding of the Alamouti code is performed by applying the complex conjugate operator on the received signal corresponding to the second component of the codeword

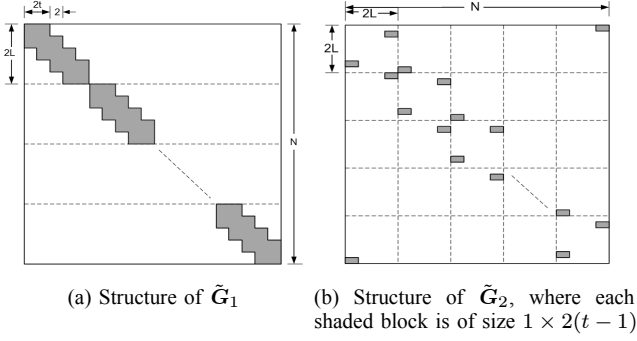


Fig. 4: Structure of the two matrices  $\tilde{\mathbf{G}}_1$  and  $\tilde{\mathbf{G}}_2$ .

followed by maximal ratio combining. Hence, we first rearrange the frequency domain received vector  $\mathbf{Y}$  to make the two components of the same codeword adjacent (reversing the separation that was done at the transmitter) and apply the conjugate operation on the even entries of the rearranged vector. The resulting  $N \times 1$  vector  $\tilde{\mathbf{Y}}$  is given by

$$\tilde{\mathbf{Y}} = \mathbf{P}_1^T \mathbf{Y} + \bar{\mathbf{P}}_1^T \mathbf{Y}^* \quad (15)$$

where the matrix  $\mathbf{P}_1^T$  ( $\bar{\mathbf{P}}_1^T$ ) selects the first (second) components of the codewords and rearranges them. By substituting from (1), (2) and (4) in (15), we can express  $\tilde{\mathbf{Y}}$  as a function of  $\mathbf{d}$  and  $\mathbf{d}^*$  as follows

$$\tilde{\mathbf{Y}} = \tilde{\mathbf{G}}_1 \mathbf{d} + \tilde{\mathbf{G}}_2 \mathbf{d}^* + \tilde{\mathbf{U}} \quad (16)$$

where

$$\tilde{\mathbf{G}}_1 = \mathbf{P}_1^T (\mathbf{G}^{(1)} \mathbf{P}_1 + \mathbf{G}^{(2)} \bar{\mathbf{P}}_2) - \bar{\mathbf{P}}_1^T (\mathbf{G}^{(1)*} \bar{\mathbf{P}}_1 - \mathbf{G}^{(2)*} \bar{\mathbf{P}}_2) \quad (17)$$

$$\tilde{\mathbf{G}}_2 = \mathbf{P}_1^T (\mathbf{G}^{(2)} \bar{\mathbf{P}}_2 - \mathbf{G}^{(1)} \bar{\mathbf{P}}_1) + \bar{\mathbf{P}}_1^T (\mathbf{G}^{(1)*} \mathbf{P}_1 + \mathbf{G}^{(2)*} \bar{\mathbf{P}}_2) \quad (18)$$

and the  $N \times 1$  vector  $\tilde{\mathbf{U}}$  is the noise vector which is given by

$$\tilde{\mathbf{U}} = \mathbf{P}_1^T \mathbf{F} \mathbf{W} \mathbf{u} + \bar{\mathbf{P}}_1^T \mathbf{F}^* \mathbf{W}^* \mathbf{u}^*. \quad (19)$$

whose covariance matrix,  $\mathbf{C}$ , is given by

$$\mathbf{C} = \sigma^2 \left( \mathbf{P}_1^T \mathbf{F} \mathbf{W} \mathbf{W}^H \mathbf{F}^H \mathbf{P}_1 + \bar{\mathbf{P}}_1^T \mathbf{F} \mathbf{W} \mathbf{W}^H \mathbf{F}^H \bar{\mathbf{P}}_1 \right) \quad (20)$$

where we have used the fact that the expectation of  $\mathbf{u} \mathbf{u}^T$  is zero due to the circularity of the noise vector  $\mathbf{u}$ .

Due to banded structure of the equivalent channel matrices  $\mathbf{G}^{(1)}$  and  $\mathbf{G}^{(2)}$ , it can be shown that the two matrices  $\tilde{\mathbf{G}}_1$  and  $\tilde{\mathbf{G}}_2$  in (16) have the structure shown in Fig. 4a and Fig. 4b, respectively. We can see from Fig. 4a that the matrix  $\tilde{\mathbf{G}}_1$  is a block-diagonal matrix, i.e., it consists of  $N/(2L)$  diagonal sub-blocks each of size  $2L \times 2L$ . In contrast, we can see from Fig. 4b that the matrix  $\tilde{\mathbf{G}}_2$  has a few number of significant elements. In particular,  $\tilde{\mathbf{G}}_2$  can be considered as a horizontal concatenation of  $N/(2L)$  sub-matrices each of dimensions  $N \times 2L$ . Each sub-matrix contains only four blocks of significant elements that exist in the first and last  $2(t-1)$  columns only.

Let us assume that the OFDM symbol  $\mathbf{d}$  is composed of  $N/(2L)$  sub-symbols as shown in Fig. 5. If the matrix  $\tilde{\mathbf{G}}_2$  did not contain any significant elements, the block-diagonal

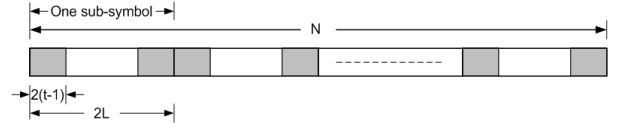


Fig. 5: Structure of the transmitted symbol  $\mathbf{d}$ .

structure of the matrix  $\tilde{\mathbf{G}}_1$  would allow the detection of each sub-symbol from the corresponding entries of the vector  $\tilde{\mathbf{Y}}$  only. In addition, the structure of each diagonal block can be exploited by using a DFE equalizer.

We propose the structure in Fig. 5 for the OFDM data symbol  $\mathbf{d}$  to overcome the problems caused by the significant entries of the matrix  $\tilde{\mathbf{G}}_2$ . According to this structure, the data symbol is divided into  $N/(2L)$  sub-symbols. Each sub-symbol contains  $2L$  elements where the first and last  $2(t-1)$  elements are pilots. Therefore, the total number of pilots within each OFDM symbol is given by  $4(t-1)N/(2L)$ . Note that these pilots can be used for example for channel estimation. Recall that the interference caused by the significant entries of  $\tilde{\mathbf{G}}_2$  arises from the first and last  $2(t-1)$  elements of each sub-symbol only. Hence, using the channel state information and the pilots, the self-interference caused by the  $\mathbf{d}^*$  in (16) can be subtracted from the received symbol  $\tilde{\mathbf{Y}}$ . For the sake of simplicity, in the remainder of this paper we will assume that the pilot symbols are guard tones, i.e., with zero value. Therefore, we can write (16) as

$$\tilde{\mathbf{Y}}^{(k)} = \tilde{\mathbf{G}}_1^{(k)} \mathbf{d}^{(k)} + \tilde{\mathbf{U}}^{(k)} \quad \forall k = 1, \dots, \frac{N}{2L} \quad (21)$$

where  $\mathbf{d}^{(k)}$  is the  $k$ th sub-symbol,  $\tilde{\mathbf{G}}_1^{(k)}$  is the  $k$ th diagonal sub-block of the matrix  $\tilde{\mathbf{G}}_1$  whose size is  $2L \times 2L$ , i.e.,

$$\tilde{\mathbf{G}}_1^{(k)}(m, n) = \tilde{\mathbf{G}}_1(m + 2L(k-1), n + 2L(k-1)) \quad (22)$$

and the  $2L \times 1$  vectors  $\tilde{\mathbf{Y}}^{(k)}$  and  $\tilde{\mathbf{U}}^{(k)}$  are the vectors containing  $2L$  entries starting from the  $(1 + 2L(k-1))$ th entry of  $\tilde{\mathbf{Y}}$  and  $\tilde{\mathbf{U}}$ , respectively. The  $m, n$ th element of the covariance matrix  $\mathbf{C}^{(k)}$  of the vector  $\tilde{\mathbf{U}}^{(k)}$  is given by

$$\mathbf{C}^{(k)}(m, n) = \mathbf{C}(m + 2L(k-1), n + 2L(k-1)). \quad (23)$$

Next, we will consider the decoding/equalization of the data symbols within the  $k$ th sub-symbol. Since the first and last  $2(t-1)$  elements of each sub-symbol are guard elements, we can write<sup>1</sup>

$$\tilde{\mathbf{Y}}^{(k)} = \bar{\mathbf{G}}^{(k)} \bar{\mathbf{d}}^{(k)} + \tilde{\mathbf{U}}^{(k)} \quad (24)$$

where  $\bar{\mathbf{d}}^{(k)}$  is a  $2L - 4(t-1) \times 1$  vector containing the unknown data elements in the sub-symbol  $\mathbf{d}^{(k)}$  and the matrix  $\bar{\mathbf{G}}^{(k)}$  is a  $2L \times (2L - 4(t-1))$  matrix that is obtained from the matrix  $\tilde{\mathbf{G}}_1^{(k)}$  by deleting the first and last  $2(t-1)$  columns.

Using the channel state information, the decoding of the  $k$ th sub-symbol starts by MMSE estimation of the last codeword in the sub-symbol as

$$\hat{\mathbf{d}}_{(1)}^{(k)} = \mathbf{E}_{(1)} \bar{\mathbf{G}}_{(1)}^{(k)} \left( \bar{\mathbf{G}}_{(1)}^{(k)} \bar{\mathbf{G}}_{(1)}^{(k)H} + \mathbf{C}_{(1)}^{(k)} \right)^{-1} \tilde{\mathbf{Y}}_{(1)}^{(k)} \quad (25)$$

<sup>1</sup>Equation (24) can be easily modified in the case of using pilots instead of guard elements by subtracting their effect from  $\tilde{\mathbf{Y}}^{(k)}$ .

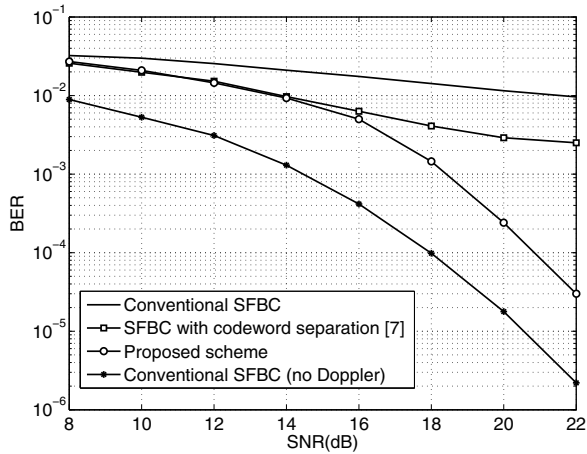


Fig. 6: BER curve for the proposed SFBC-OFDM (Doppler=25%)

where  $\tilde{\mathbf{G}}_{(1)}^{(k)}$  is the  $2(t+1) \times 2(t+1)$  matrix composed of the last  $2(t+1)$  rows and columns in  $\tilde{\mathbf{G}}^{(k)}$ ,  $\tilde{\mathbf{Y}}_{(1)}^{(k)}$  is a  $2(t+1) \times 1$  vector containing the last  $2(t+1)$  entries in the vector  $\tilde{\mathbf{Y}}^{(k)}$ ,  $\hat{\mathbf{d}}_{(1)}^{(k)}$  is the estimated value of the data in the last codeword in  $\tilde{\mathbf{d}}^{(k)}$ ,  $\mathbf{E}_{(1)} = [\mathbf{0}_{(2,2t)}, \mathbf{I}_2]$  and the  $2(t+1) \times 2(t+1)$  matrix  $\mathbf{C}_{(1)}^{(k)}$  is the covariance matrix of the last  $2(t+1)$  entries in  $\tilde{\mathbf{U}}^{(k)}$ , which contributes to  $\tilde{\mathbf{Y}}_{(1)}^{(k)}$  and is given by the last  $2(t+1)$  rows and columns of  $\mathbf{C}^{(k)}$ . After estimating the last codeword in  $\tilde{\mathbf{d}}^{(k)}$ , the decision on this codeword can be fed back to cancel the contribution of this codeword to  $\tilde{\mathbf{Y}}^{(k)}$  using the last two columns of  $\tilde{\mathbf{G}}^{(k)}$ . The rest of the codewords are estimated using the same procedure.

## V. SIMULATION RESULTS

We consider an OFDM system with  $N = 1024$  subcarriers and 10 MHz bandwidth employing an Alamouti SFBC. The data bits are modulated using QPSK modulation. We consider an urban channel with TU-06 delay profile defined by the COST 207 project where each discrete channel tap is generated by an independent complex Gaussian random variable with time correlation based on Jakes model. In these simulations we use  $t = 2$  and  $L = 16$ . Also, based on simulations, the window is not efficient when  $t = 1$ .

We compare the performance of the proposed algorithm with that of the conventional SFBC and the SFBC-OFDM with separation and 3-taps MMSE equalizer proposed in [7]. The channel is time-varying with normalized Doppler shift equal to 0.25 and perfect channel knowledge is assumed for all algorithms. As a lower bound on the bit error rate (BER) performance, we also consider a conventional SFBC-OFDM system operating in a static channel (without Doppler). Fig. 6 shows the BER versus the received signal to noise ratio (SNR). We can see from this figure that the conventional SFBC fails completely even at high SNR due to the relatively high Doppler shift. We can also see that separating the codeword components is not sufficient to overcome the ICI for this high value of the Doppler shift. In contrast, the proposed scheme

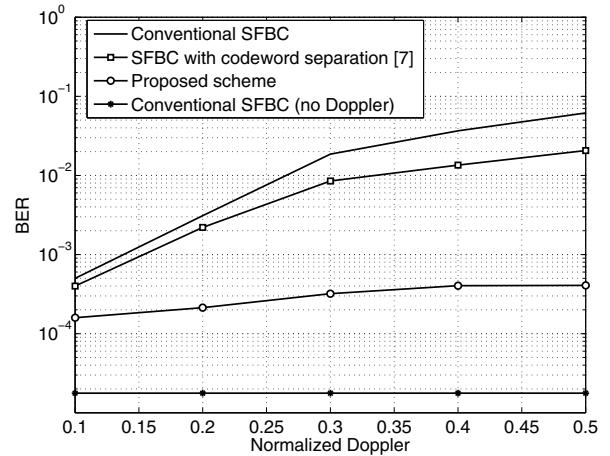


Fig. 7: BER curves versus Doppler shift (SNR=20 dB)

preserves the diversity gain which is evident from the similarity between the high SNR BER slopes for the proposed scheme and the conventional receiver with no Doppler. Fig. 7 shows the performance of different schemes versus the normalized Doppler at an SNR of 20 dB. We can see from this figure that in contrast with earlier approaches, the proposed scheme can combat high values of the Doppler shift and that the BER does not rise catastrophically as the Doppler shift increases.

## VI. CONCLUSION

High mobility degrades the performance of SFBC-OFDM due to ICI that destroys the orthogonality between sub-carriers. We have proposed an optimal windowing technique at the receiver that limits the ICI to a limited number of neighboring sub-carriers. In addition, the codeword components are separated within the coherence bandwidth by a number of sub-carriers larger than the range of ICI. We have also proposed an MMSE-based DFE equalizer with that reduces the equalization complexity. Simulation results have been presented that illustrate the improved performance of the proposed scheme even in doubly-selective channels with very high Doppler.

## REFERENCES

- [1] C. Mecklenbrauker, A. Molisch, J. Karedal, F. Tufvesson, A. Paier, L. Bernado, T. Zemen, O. Klemp, and N. Czink, "Vehicular channel characterization and its implications for wireless system design and performance," in *Proc. IEEE*, vol. 99, no. 7, pp. 1189–1212, Jul. 2011.
- [2] J. A. C. Bingham, "Multicarrier modulation for data transmission: An idea whose time has come," in *IEEE Communications Magazine*, vol. 28, May 1990, pp. 5–14.
- [3] S. Lu, R. Kalbasi, and N. Al-Dhahir, "OFDM interference mitigation algorithms for doubly-selective channels," in *Proc. of Vehicular Technology Conference (VTC)*, Sep. 2006, pp. 1–5.
- [4] P. Schniter and S. D'Silva, "Low-complexity detection of OFDM in doubly-dispersive channels," in *Proc. Asilomar Conference on Signals, Systems and Computers*, vol. 2, Nov. 2002, pp. 1799–1803.
- [5] S. M. Alamouti, "A simple transmit diversity technique for wireless communications," in *IEEE Communications Magazine*, vol. 16, Oct. 1998, pp. 1451–1458.
- [6] K. Lee and D. Williams, "A space-frequency transmitter diversity technique for OFDM systems," in *Proc. GLOBECOM*, vol. 3, Nov. 2000, pp. 1473–1477.
- [7] S. Lu, B. Narasimhan, and N. Al-Dhahir, "A novel SFBC-OFDM scheme for doubly selective channels," *IEEE Transactions on Vehicular Technology*, vol. 58, no. 5, pp. 2573–2578, Jun. 2009.